

Scanning Probing of the Tribovoltaic Effect at the Sliding Interface of Two Semiconductors

Mingli Zheng, Shiquan Lin, Liang Xu, Laipan Zhu, and Zhong Lin Wang*

Contact electrification (CE or triboelectrification) is a common phenomenon, which can occur for almost all types of materials. In previous studies, the CE between insulators and metals has been widely discussed, while CE involving semiconductors is only recently. Here, a tribo-current is generated by sliding an N-type diamond coated tip on a P-type or N-type Si wafers. The density of surface states of the Si wafer is changed by introducing different densities of doping. It is found that the tribo-current between two sliding semiconductors increases with increasing density of surface states of the semiconductor and the sliding load. The results suggest that the tribo-current is induced by the tribovoltaic effect, in which the electron–hole pairs at the sliding interface are excited by the energy release during friction, which may be due to the transition of electrons between the surface states during contact, or bond formation across the sliding interface. The electron–hole pairs at the sliding interface are subsequently separated by the built-in electric field at the PN or NN heterojunctions, which results in a tribo-current, in analogy to that which occurs in the photovoltaic effect.

Contact electrification (CE or triboelectrification) is a very common phenomenon, which can occur for almost all types of materials, including insulators, metals and semiconductors.^[1] Since it may lead to discharge and explosion, the CE was always referred to as a negative effect, until the invention of the triboelectric nanogenerators (TENGs) that convert ubiquitous ambient mechanical energy into electricity.^[2–4] The typical TENGs are usually constructed by the insulators and the metals, and at least one of the contact pairs is insulator, so that the charges can stay on the surface and induce the displacement current.^[5] Recently, it was found that the CE will be very different when the semiconductor is involved.^[6] The current

can be generated by the contact or sliding of a P-type semiconductor against an N-type semiconductor^[7–9] (or semiconductor against metal^[10–12]), and a novel electric generator was proposed.^[7] This new type of electric generator is gaining attention for that a direct current can be generated without a rectifier module.^[8–11] However, the mechanism of the current generation in the CE involving semiconductors is still under debate.

For the contact between a P-type semiconductor and an N-type semiconductor, the PN junction will be formed at the interface.^[13,14] It is highly suspected that the built-in electric field in the PN junction makes the CE between the semiconductors different from that between conventional materials. Considering that, Wang et al. pointed out that the generation of the continuous direct current induced by the sliding of P-type semiconductor against


N-type semiconductor is similar to the photovoltaic effect, and can be referred to as the “tribovoltaic effect.”^[15] The only difference is that the electron–hole pairs in tribovoltaic effect are excited during friction, in which the energy is released due to either the transition of electrons from the surface states of one side to that of another side in the contact or sliding,^[16–21] or the energy released while forming a new bond at the interface,^[22] just as it occurs in the CE between two conventional materials.^[23–26] Then, the electron–hole pairs are separated by the built-in electric field and the external current flowing from the P-side to the N-side will be induced, as it occurs in the photovoltaic effect.^[27–29] According to the tribovoltaic effect, the excitation efficiency of electron–hole pairs highly depends on the density of surface states of the semiconductors and the bonding interactions. Hence, the tribovoltaic current may be related to the density of surface states of the semiconductors and the sliding load, which can significantly affect the bonding interactions at the sliding interface.^[22]

In this work, the direct current is generated by sliding an N-type semiconductor tip over a Si sample surface using conductive atomic force microscopy (CAFM).^[30,31] Both P-type and N-type Si samples with various doping concentrations are used in the experiments. Further, the Si samples are treated by inductively coupled plasma reactive ion etching (ICP-RIE), which can significantly increase the density of surface states of the semiconductors by doping or introducing defects on the surface.^[32,33] It is revealed that the current density in the sliding experiments increases with increasing of the density of surface

Dr. M. Zheng, Dr. S. Lin, Prof. L. Xu, Prof. L. Zhu, Prof. Z. L. Wang
Beijing Institute of Nanoenergy and Nanosystems
Chinese Academy of Sciences
Beijing 100083, P. R. China
E-mail: zlwang@gatech.edu

Dr. M. Zheng, Dr. S. Lin, Prof. L. Xu, Prof. L. Zhu, Prof. Z. L. Wang
School of Nanoscience and Technology
University of Chinese Academy of Sciences
Beijing 100049, P. R. China

Prof. Z. L. Wang
School of Materials Science and Engineering
Georgia Institute of Technology
Atlanta, GA 30332-0245, USA

 The ORCID identification number(s) for the author(s) of this article can be found under <https://doi.org/10.1002/adma.202000928>.

DOI: 10.1002/adma.202000928

states of the Si samples, which is consistent with the proposed mechanism of the tribovoltaic effect. The effect of sliding load on the tribo-current is also discussed. Moreover, the conductive tip is also used to rub the Si samples, and the results suggest that the tribovoltaic effect can occur not only in the PN junction, but also in the Schottky junction.

Here, the nitrogen-doped diamond coated tip is used as the N-type semiconductor in the contact pair for its good wear-resistive performance. The samples are the boron or phosphorus doped Si with different resistivities, which corresponds to different doping concentrations. As shown in Figure 1a, the diamond coated tip was controlled to rub on the Si sample with a certain load. During the rubbing, the current between the tip and sample was recorded in the conductive atomic force microscopy (CAFM) mode (the external current flowing from the sample to the tip is defined as positive). If the Si sample is P-type doped, the PN junction will be formed due to the diffusion of the electrons from the N-side to the P-side at the interface, as shown in the inset of Figure 1a. The current–voltage curve between the diamond coated tip and the P-type

Si sample ($10\text{--}20\ \Omega\ \text{cm}$) was measured, and the results show the rectification performance of the interface between the tip and the sample, as shown in Figure 1b. It is suggested that the PN heterojunction and the built-in electric field was formed at the interface when the tip contact the P-type Si sample ($10\text{--}20\ \Omega\ \text{cm}$), and the energy band diagram of the PN heterojunction at the N-type diamond and P-type Si interface can be described as that in the inset of Figure 1b.

Figure 1c gives the tribo-current between the diamond coated tip and the Si samples with different doping concentrations, when the tip scans on the sample surface with a 1000 nN load. The current maps for different Si samples are shown in the inset of Figure 1c, and typical sections of current value are also given. It can be seen that the positive current (flowing from the sample to the tip in the external circuit) is generated between the tip and P-type Si samples with $0.1\text{--}0.5\ \Omega\ \text{cm}$ and $10\text{--}20\ \Omega\ \text{cm}$ resistivity. These results are consistent with the proposed mechanism of the tribovoltaic effect, in which the external tribo-current should flow from the P-side to the N-side. Also,

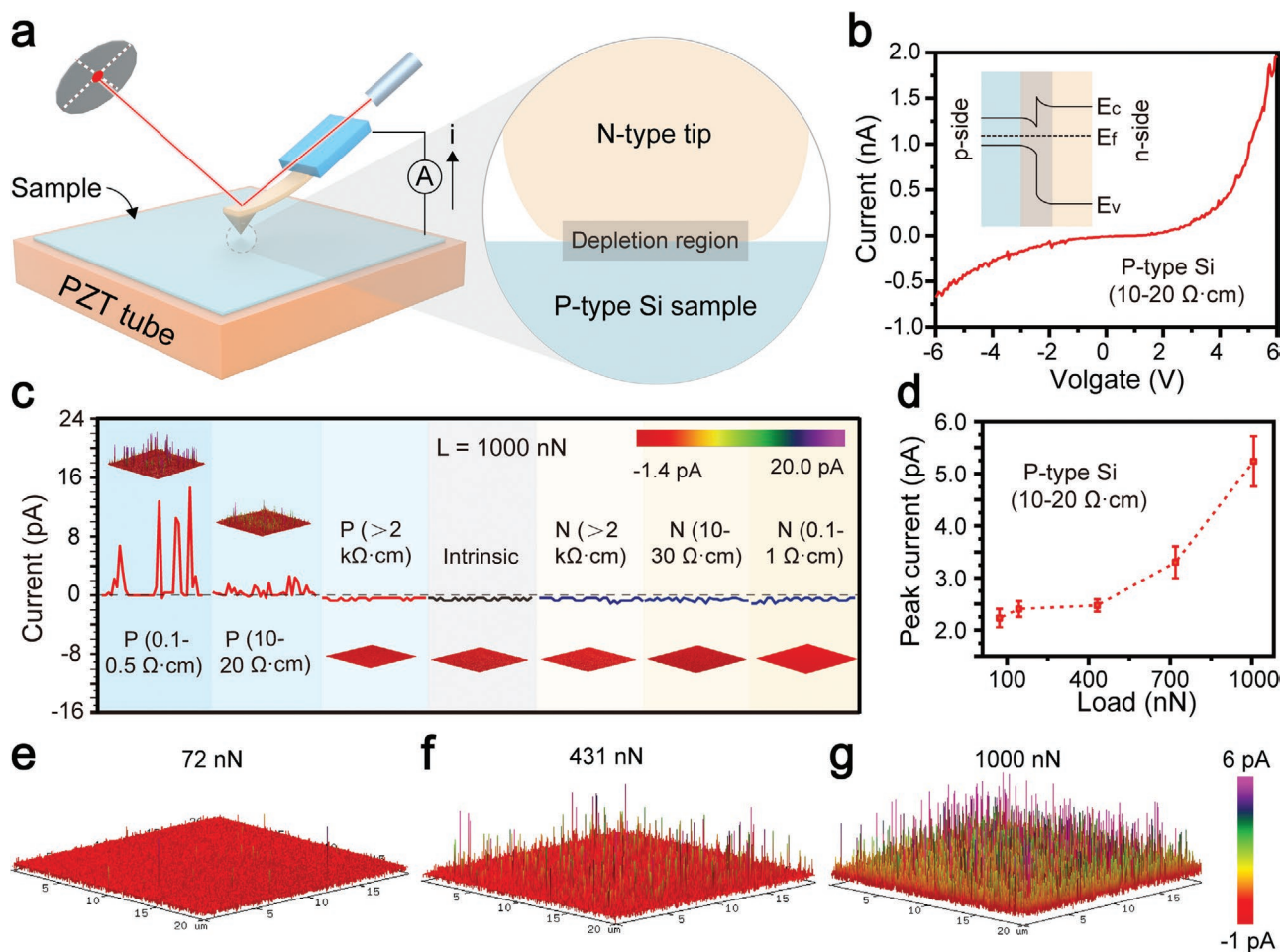


Figure 1. Schematic illustration of CAFM experiments. a) The setup of CAFM experiment platform. b) Current–voltage curves between N-type diamond coated tip and P-type Si with $10\text{--}20\ \Omega\ \text{cm}$ resistivity (the tip is grounded and the bias is applied on the sample). c) The tribo-current between the N-type diamond coated tip and Si samples with different doping types and concentrations under 1000 nN sliding load. d) The effect of sliding load on the tribo-current between N-type diamond coated tip and P-type Si with $10\text{--}20\ \Omega\ \text{cm}$ resistivity. The current maps when the N-type diamond coated tip scans a P-type Si with $10\text{--}20\ \Omega\ \text{cm}$ resistivity under e) 72 nN, f) 431 nN, and g) 1000 nN sliding load. (E_c is the bottom of the conduction band, E_f is the Fermi level and E_v is the top of the valence band.)

there is no current observed when the Si samples are N-type doped or the P-type doping concentration is not high enough, probably because the built-in field in the NN heterojunction is too weak to separate all the electron-hole pairs at the interface. The effect of the sliding load on the tribo-current was also investigated here. The relation between the sliding load and the peak current in the maps is given in Figure 1d, and the maps of the tribo-current between the tip and P-type Si with 10–20 Ω cm resistivity under different sliding loads are shown in Figure 1e,g. The peak current is found to be increased with the increasing load, which is easy to understand because the contact area will be larger under a higher load. But interestingly, the number of current peaks also increases with the load in the maps, as shown in the Figure 1e,g. When the sliding load is 72 nN (Figure 1e), the current peaks are very sparse, and they become tightly spaced when the sliding load increases to 1000 nN (Figure 1g). This is unlikely to be caused by the increased contact area, because the contact area can only increase the height of peak current, but not the density of current peaks. Hence, it indicates that the tribo-current is more easily to be generated under a high sliding load, which may be caused by the stronger bonding interactions under a higher sliding load.

The density of surface states of the contact pair is one of the most important factors affecting the amount of the tribo-excited electrons. Here, the ICP-RIE treatment is performed to increase the density of surface states of the Si wafer,^[32,33] and the effect of density of surface states on the tribo-current is discussed. Figure 2a shows a schematic diagram of ICP-RIE

treatment, in which SF₆, O₂, and Ar are the reaction gases. The X-ray photoelectron spectra of the ICP-RIE treated Si samples are shown in Figure S1 in the Supporting Information, the samples were not significantly changed except that trace amount of fluorine and sulfur elements were detected on the Si surfaces. The tribo-current between the diamond coated tip and the ICP-RIE treated Si samples were measured, and the results are given in Figure 2b. It is obvious that the tribo-current between the tip and Si samples increased significantly. For the P-type Si with 0.1–0.5 Ω cm resistivity, the highest current peak increases from \approx 16 pA to \approx 55 pA after the ICP-RIE treatment, when even a smaller sliding load (110 nN) was applied. For the P-type Si with >2 k Ω cm resistivity, intrinsic Si and even N-type Si samples, which cannot generate current by rubbing with the tip before the ICP-RIE treatment, the tribo-current was also observed after the treatment. Furthermore, the tribo-current is positive when the sample is P-type doped, and reverses to be negative when the sample is N-type doped. The reversion is probably because the direction of the built-in electric field will be reversed in the NN heterojunction.

In order to test the PN and NN heterojunctions at the interface after the treatment, the current-voltage curves between the tip and different ICP-RIE treated Si samples were measured. For the P-type Si with 10–20 Ω cm resistivity (as shown in Figure 2c), the rectification performance become worse comparing to the curve before the ICP-RIE treatment (Figure 1b), which may be caused by the doping of fluorine and sulfur atoms in the ICP-RIE treatment. The current-voltage curve of the NN heterojunction at the interface between the tip and N-type Si

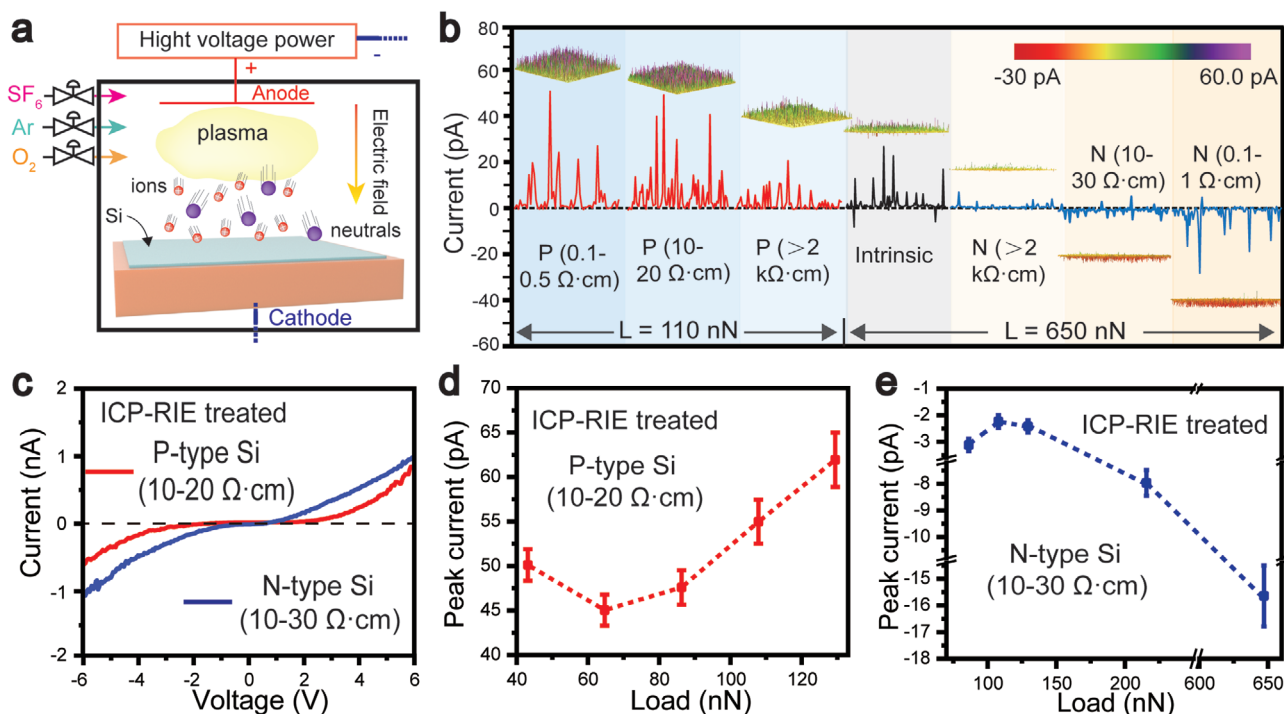


Figure 2. Effects of the ICP-RIE treatment on the tribo-current between the tip and Si. a) The setup of the ICP-RIE treatment. b) The tribo-current between the N-type diamond coated tip and ICP-RIE treated Si samples with different doping types and concentrations. c) Current–voltage curves between an N-type diamond coated tip and ICP-RIE treated P-type/N-type Si samples. d,e) The effect of sliding load on the tribo-current between an N-type diamond coated tip and ICP-RIE treated p-type Si with 10–20 Ω cm resistivity (d), and n-type Si with 10–30 Ω cm resistivity (e).

with 10–30 Ω cm resistivity is also shown in Figure 2c, and the current–voltage curves for other N-type Si samples are shown in Figure S2 in the Supporting Information. It can be seen that the rectification performance of the NN heterojunctions are all very weak. These results suggest that the increase of tribo-current is not caused by the increased strength of the built-in electric field. Hence, the increase of the density of surface states of the Si samples is most probable responsible for the increased tribo-current. The effects of the sliding load on the peak current between the tip and P-type Si (10–20 Ω cm resistivity), N-type Si (10–30 Ω cm resistivity) are shown in Figure 2d,e (and the relations for other samples are shown in Figure S3 in the Supporting Information). The results show that the peak current decreases first and then increases with the sliding load for all the Si samples. In addition, the density of the current peaks increases with the increasing sliding load for both P-type and N-type Si samples (Figures S4 and S5, Supporting Information), which implies that the bonding interactions can promote the generation of tribo-current between two sliding semiconductors. Here, the increase of the density of the current peaks implies that the charges or energy at the interface between the tip and the sample will be released in a larger area with a larger

sliding load. Hence, the peak current decreases first (when the sliding load is small) since the charges flow away in a larger area. With the increase of the sliding load, the bonding interactions between the tip and sample increase significantly, the peak current increase with the sliding load though the increase of the density of current peaks.

Based on the results, the mechanism of the generation of tribo-current can be described as the tribovoltaic effect. The effects of ICP-RIE treatment and sliding load on the tribo-current can also be explained. As shown in Figure 3a, the Fermi level of the N-type diamond coated tip is higher than the P-type Si samples, and there are electrons in the surface states of the semiconductors (in the energy band diagram, the value of the Si gap is 1.1 eV and diamond is 5.5 eV, and the work function of Si is about 4.75 eV and diamond is 3.2 eV). When they come into contact, the electrons will diffuse from the N-side to the P-side (holes will diffuse in the opposite direction), and the PN heterojunction will be formed. In the meantime, electrons trapped in the high energy level surface states on the N-type semiconductor will transit to the surface states on the P-type semiconductor, and energy will be released due to the transition of the electrons, as shown in Figure 3b (this step is exactly the same

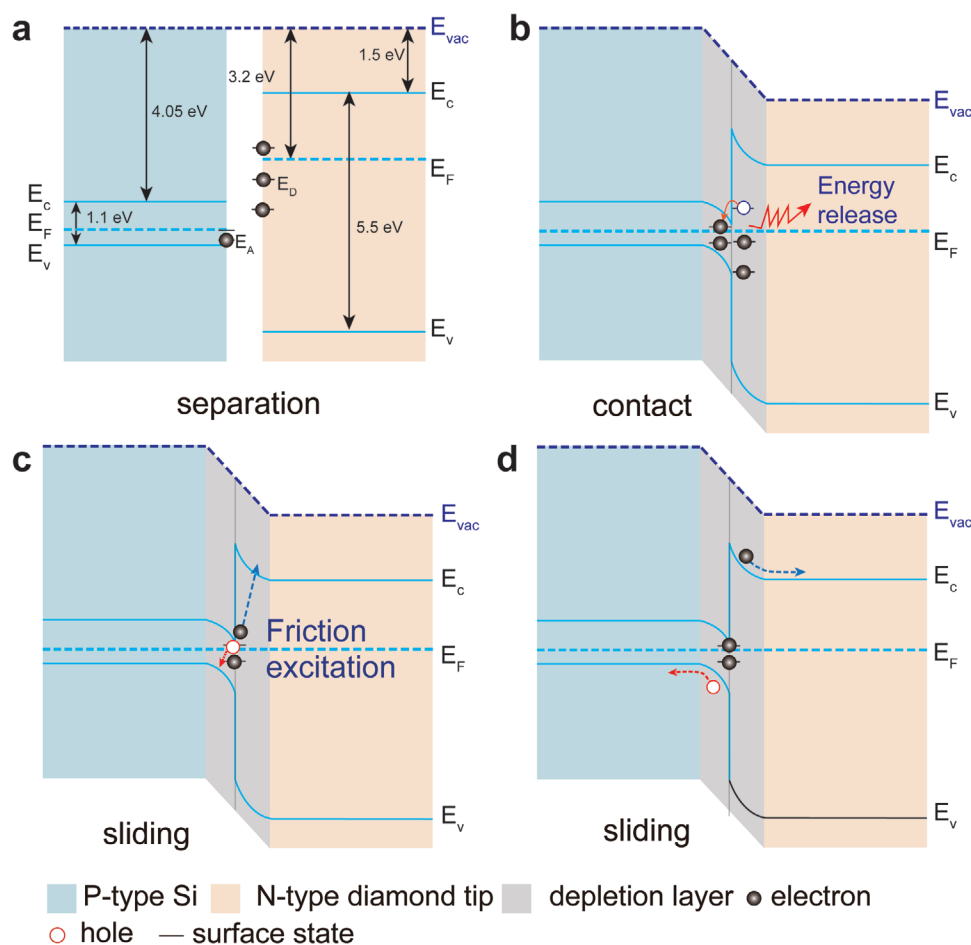


Figure 3. Energy band diagram of tribovoltaic effect at a PN heterojunction. a–c) Energy band diagrams of the P-type semiconductor and N-type semiconductor before contact (a), in contact (b), and in sliding (c). d) The movement of the electrons and holes at the PN heterojunction interface in sliding. (E_c is the bottom of the conduction band, E_f is the Fermi level and E_v is the top of the valence band, E_A is the energy level of the acceptor states and E_D is the energy level of the donor states).

with the CE between the conventional materials). The electron–hole pairs at the interface will be excited by the released energy, provided the energy released is enough to excite the electron–hole pairs at the interface (Figure 3c). It may be noted that the energy required to excite the electron–hole pair at the interface may be significantly lower than that for exciting e-h in the valence band of either the P side or the N side, because of the existence of surface states at the PN junction. On the other hand, energy can also be released by the newly formed bonds at the PN junction due to sliding-contacting, which may also excite the electron–hole pairs. Driven by the built-in electric field in the PN heterojunction, the electrons will move to the N-side and the holes will move to the P-side, and the external tribo-current flowing from the P-side to the N-side in the outer circuit is induced (Figure 3d). When the Si samples are ICP-RIE treated, the density of surface states of the Si sample will increase and more electrons will transit between the surface states, leading to more energy release and exciting more electron–hole pairs. Also, the increasing of sliding load may result in stronger bonding interactions, and increase the generation efficiency of the electron–hole pairs. Hence, the tribo-current is easier to be induced under high sliding load, and the ICP-RIE treatment can lead to higher tribo-current.

Comparing to the PN heterojunction, the strength of the built-in electric field in the NN heterojunction at the interface between the tip and sample is weaker. Only a small proportion of the electrons–hole pairs can be separated by the built-in electric field. Hence, no current was detected between the tip and untreated N-type Si samples, since the density of surface states cannot produce enough electron–hole pairs to generate observable current at this condition. After the ICP-RIE treatment, the density of the surface states of the Si sample is rapidly increased, and the energy band diagram for the tribovoltaic effect in the NN heterojunction after the ICP-RIE treatment is shown in Figure S6 in the Supporting Information. The band structure of the Si sample and the tip before contact is shown in Figure S6a in the Supporting Information. Affected by the surface states, the band offsets of the Si sample and the tip at the interface will be both positive (upward) when they contact each other,^[34–36] as shown in Figure S6b in the Supporting Information. The electrons at the surface states will be excited due to the friction excitation (Figure S6b, Supporting Information). Because the density of the surface states of the Si sample is increased by the ICP-RIE treatment, many electron–hole pairs will be generated at the Si side, and the electrons will flow from the interface to the Si side induced by the built-in electric field, and negative tribo-current will be generated.

Furthermore, the tribo-current between the Pt tip and Si samples is also observed, which means that the tribovoltaic effect can also occur at a Schottky junction. Figure 4a,b shows the current–voltage between the Pt tip and the P-type Si with 0.1–0.5 Ω cm resistivity, N-type Si with 10–30 Ω cm resistivity, respectively. The interfaces showed good rectification performance. It implies that the Schottky junction is formed at the interface of the Pt tip and Si samples. It is shown that the tribo-current can also be generated between the Pt and Si samples in Figure 4c. But the tribo-current is very small, since the density of surface states of the untreated Si samples is quite low. After the ICP-RIE treatment, the current–voltage curves between the

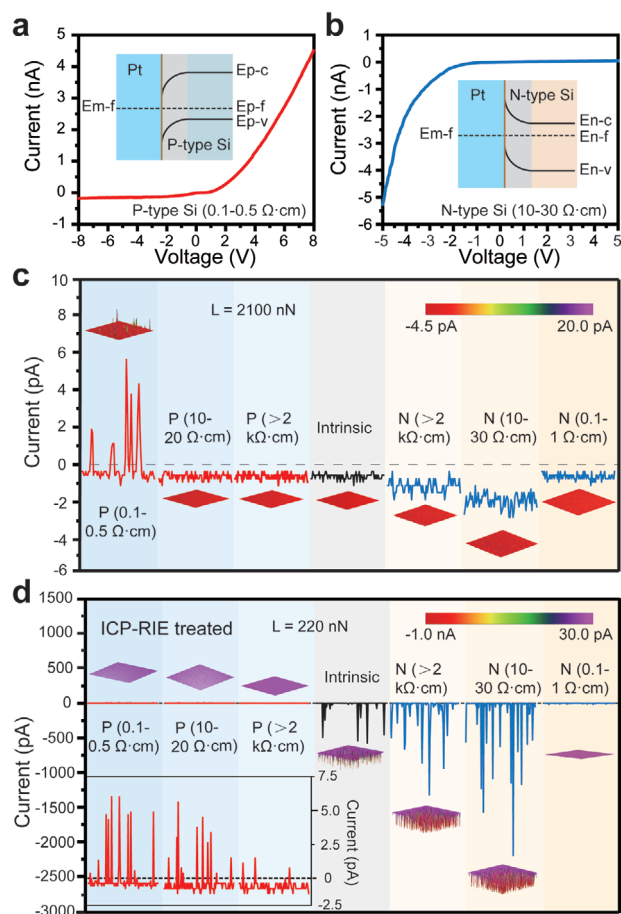


Figure 4. The tribo-current between Pt tip and Si samples with different doping types and concentrations. a,b) Current–voltage curves between Pt coated tip and P-type (a) and N-type (b) Si samples. c,d) The tribo-current between the Pt coated tip and the Si samples (c) and the ICP-RIE-treated Si samples (d) with different doping types and concentrations.

Pt tip and both the P-type and N-type Si are given in Figure S7 in the Supporting Information. It can be seen that the rectification performance of the Schottky junction got slightly worse comparing to that in the Figure 4a,b, which means that the built-in electric field become weaker after the ICP-RIE treatment. But the tribo-current between the Pt tip and Si samples is significantly increased by the ICP-RIE treatment, as shown in Figure 4d. Especially for the N-type Si samples, the peak tribo-current can even be up to -2000 pA after the ICP-RIE treatment. This is most probable caused by the increase of the density of surface states of the Si sample due to the ICP-RIE treatment. For the P-type Si samples, the tribo-current is only slightly increased. We think this is possibly because that the P-type Si is hole redundant, and the charge carrier in the P-type Si are holes, which have larger effective mass than that of electrons. Hence, the response of the metal/P-type Si interface to the friction excitation is slower than that of the metal/N-type Si interface, and lead to the low tribo-current and low sensitivity to the density of surface states. It is also noted that the tribo-current between the Pt tip and N-type Si with 0.1–1 Ω cm resistivity is very low. Here, the poor rectification performance (Figure S8, Supporting Information) suggests that the contact of Pt tip and

N-type Si with 0.1–1 Ω cm resistivity is close to Ohmic contact, due to the over doping of the N-type Si.

In the tribovoltaic effect, the transition of the electrons trapped in the surface states is very important for the first step, in which the energy is released to excite the electron–hole pairs. This step in the tribovoltaic effect gives a hint to the study of the CE. It suggests that the electron trapped in the surface states of the materials is the charge carriers in the CE. So far, the tribovoltaic effect has already been used to harvest mechanical energy, similar to the photovoltaic effect for solar energy harvesting. An important feature of the electric generator based on tribovoltaic effect is that the direct current can be generated. Hence, the electric generator based on tribovoltaic effect is an important complement to the conventional TENGs, which usually generate an alternating current.

In conclusion, a direct current is generated by sliding the N-type diamond coated tip over the Si samples with different doping concentrations. The density of surface states of the Si samples was increased by the ICP-RIE treatment. It is revealed that the tribo-current between the Si samples increase with the increasing density of surface states of the Si sample and the sliding load. The results suggest that the tribo-current between two semiconductors (or semiconductor and metal) is induced by the tribovoltaic effect, in which the electron–hole pairs at the interface may be excited by the energy release due to the transition of electrons from the surface states of one semiconductor to that of another, and also by the energy released from bond formation across the sliding interface. Further, the electron–hole pairs are separated by the built-in electric field at the PN, NN, and Schottky junctions, inducing the observed current. This is the first time, to our best knowledge, that the tribovoltaic effect is clearly described and verified experimentally. Our findings also provide a method to enhance the output current in the electric generator based on the tribovoltaic effect.

Experimental Section

ICP-RIE Treatment: The ICP-RIE treatment was carried out on the commercial ICP-RIE equipment SI 500 (Sentech Instruments GmbH, Germany). The flow rate of the SF₆, O₂, and Ar was 30, 5, and 10 standard-state cubic centimeter per minute, respectively. The etching treatment was remained for 60 s.

CAFM Experiments: The CAFM experiments were all performed on a commercial AFM equipment Icon (Bruker, USA). DCP 01 (NT-MDT&Tipsnano, Russia) was used as the N-type diamond coated tip and the Pt tip was 25Pt400B (RockyMountain Nanotechnology, USA). In the CAFM scanning, the scan size was 20 μ m and scan rate was 1 Hz. It needs to be noted that the external current flowing from the sample to the tip is defined as positive during the CAFM scanning, but it is defined as negative in the current–voltage curve measurement.

Supporting Information

Supporting Information is available from the Wiley Online Library or from the author.

Acknowledgements

M.Z. and S.L. contributed equally to this work. Research was supported by the National Key R & D Project from Minister of Science and

Technology (2016YFA0202704), National Natural Science Foundation of China (Grant Nos. 51605033 and 51432005), and Beijing Municipal Science & Technology Commission (Z171100002017017, Y3993113DF).

Conflict of Interest

The authors declare no conflict of interest.

Keywords

conductive atomic force microscopy, contact electrification, electron transfer, semiconductors, tribovoltaic effect

Received: February 10, 2020

Revised: March 16, 2020

Published online:

- [1] J. Lowell, A. C. Rose-Innes, *Adv. Phys.* **1980**, *29*, 947.
- [2] F. Fan, Z. Tian, Z. L. Wang, *Nano Energy* **2012**, *1*, 328.
- [3] Z. L. Wang, J. Chen, L. Lin, *Energy Environ. Sci.* **2015**, *8*, 2250.
- [4] R. Hinchet, H. Yoon, H. Ryu, M. Kim, E. Chol, D. Kim, S. Kim, *Science* **2019**, *365*, 491.
- [5] Z. L. Wang, *Nano Energy* **2020**, *68*, 104272.
- [6] Q. Zhang, R. Xu, W. Cai, *Nano Energy* **2018**, *51*, 698.
- [7] R. Xu, Q. Zhang, J. Wang, D. Liu, J. Wang, Z. L. Wang, *Nano Energy* **2019**, *66*, 104185.
- [8] Y. Lu, Z. Hao, S. Feng, R. Shen, Y. Yan, S. Lin, *iScience* **2019**, *22*, 58.
- [9] Y. Lu, S. Feng, R. Shen, Y. Xu, Z. Hao, Y. Yan, H. Zheng, X. Yu, Q. Gao, P. Zhang, S. Lin, *Research* **2019**, *2019*, 5832382.
- [10] S. Lin, Y. Lu, S. Feng, Z. Hao, Y. Yan, *Adv. Mater.* **2019**, *31*, 1804398.
- [11] J. Liu, A. Goswami, K. Jiang, F. Khan, S. Kim, R. McGee, Z. Li, Z. Hu, J. Lee, T. Thundat, *Nat. Nanotechnol.* **2018**, *13*, 112.
- [12] J. Liu, M. Miao, K. Jiang, F. Khan, A. Goswami, R. McGee, Z. Li, L. Nguyen, Z. Hu, J. Lee, K. Cadien, T. Thundat, *Nano Energy* **2018**, *48*, 320.
- [13] X. Yu, T. Marks, A. Facchetti, *Nat. Mater.* **2016**, *15*, 383.
- [14] H. Ohta, N. Kaneda, F. Horikiri, Y. Narita, T. Yoshida, T. Mishima, T. Nakamura, *IEEE Electron Device Lett.* **2015**, *36*, 1180.
- [15] Z. L. Wang, A. C. Wang, *Mater. Today* **2019**, *30*, 34.
- [16] M. Willatzen, Z. L. Wang, *Nano Energy* **2018**, *52*, 517.
- [17] J. Lowell, *J. Phys. D: Appl. Phys.* **1976**, *9*, 1571.
- [18] B. Hamilton, A. Rose-Innes, *J. Electrostat.* **1981**, *10*, 121.
- [19] W. Pong, D. Brandt, Z. He, W. Imano, *J. Appl. Phys.* **1985**, *58*, 896.
- [20] B. Kwetkus, K. Sattler, *J. Phys. D: Appl. Phys.* **1992**, *25*, 1400.
- [21] M. Jean, S. Hudlet, C. Guthmann, J. Berger, *Eur. Phys. J. B* **1999**, *12*, 471.
- [22] G. Pezzotti, C. Camara, E. Marin, W. Zhu, D. Green, A. Collins, S. Putterman, *J. Mater. Chem. C* **2019**, *7*, 7708.
- [23] C. Xu, Y. Zi, A. Wang, H. Zou, Y. Dai, X. He, P. Wang, Y. Wang, P. Feng, D. Li, Z. L. Wang, *Adv. Mater.* **2018**, *30*, 1706790.
- [24] S. Lin, L. Xu, C. Xu, X. Chen, A. Wang, B. Zhang, P. Lin, Y. Yang, H. Zhao, Z. L. Wang, *Adv. Mater.* **2019**, *31*, 1808197.
- [25] S. Lin, L. Xu, L. Zhu, X. Chen, Z. L. Wang, *Adv. Mater.* **2019**, *31*, 1901418.
- [26] J. Lowell, *J. Phys. D: Appl. Phys.* **1977**, *10*, 65.
- [27] B. Baugher, H. Churchill, Y. Yang, P. Jarillo, *Nat. Nanotechnol.* **2014**, *9*, 262.
- [28] M. Buscema, D. Groenendijk, G. Steele, H. van der Zant, A. Castellanos, *Nat. Commun.* **2014**, *5*, 4651.
- [29] X. Zhan, A. Facchetti, S. Barlow, T. Marks, M. Ratner, M. Wasielewski, S. Marder, *Adv. Mater.* **2011**, *23*, 268.

- [30] J. Seidel, P. Maksymovych, Y. Batra, A. Katan, S. Yang, Q. He, A. Baddorf, S. Kalinin, C. Yang, J. Yang, Y. Chu, E. Salje, H. Wormeester, M. Salmeron, R. Ramesh, *Phys. Rev. Lett.* **2010**, *105*, 197603.
- [31] V. Garcia, S. Fusil, K. Bouzehouane, S. Enouz-vedrenne, N. Mathur, A. Barthelemy, M. Bibes, *Nature* **2009**, *460*, 81.
- [32] I. Kim, K. Chol, J. Lee, *J. Vac. Sci. Technol., B* **2005**, *23*, 495.
- [33] W. Lan, K. Huang, K. Huang, *Solid-State Electron.* **2006**, *50*, 11.
- [34] G. Amaratunga, *Appl. Phys. Lett.* **1991**, *59*, 69.
- [35] W. Ni, J. Knall, G. Hansson, *Phys. Rev. B* **1987**, *36*, 7744.
- [36] W. Frensley, H. Kroemer, *Phys. Rev. B* **1977**, *16*, 2642.